Domain faceting in an in-plane magnetic reorientation transition

E. Vescovo,[1] T. O. Menteş,[2] J. T. Sadowski,[3] J. M. Ablett,[4] M. A. Niño,[2] and A. Locatelli[2]
[1]*National Synchrotron Light Source, Brookhaven National Laboratory, Upton, New York 11973, USA*
[2]*Sincrotrone Trieste S.C.p.A., Basovizza, Trieste 34149, Italy*
[3]*Center for Functional Nanomaterials, Brookhaven National Laboratory, Upton, New York 11973, USA*
[4]*Synchrotron Soleil, L'orme des Merisiers, Saint-Aubin, BP 48, Gif-sur-Yvette F-91192, France*
(Received 21 September 2010; published 4 November 2010)

The microscopic structure of the 90° *in-plane* magnetic reorientation transition in Fe(110) films is examined using photoemission x-ray microscopy. At the nanoscale, sharp magnetic boundaries are detected. They are indicative of a first-order transition and are consistent with Fe magnetic anisotropy constants. At the micron scale, the magnetic boundary breaks up into triangular patterns whose characteristic angular dependence is revealed by experiments on conical microwedges. This effect, fully accounted by micromagnetic simulations, opens the possibility to control the sharpness of the transition at the microscopic scale.

DOI: 10.1103/PhysRevB.82.184405 PACS number(s): 64.60.Ej, 05.70.Jk, 68.37.Nq

I. INTRODUCTION

The breaking of the three-dimensional symmetry manifests dramatically in the magnetic properties of thin films.[1] The most striking phenomena, as the development of magnetic moments in quasi-two-dimensional (2D) systems,[2] are known to occur at the ultrathin-film limit.[3] A common feature often accompanying three-dimensional to 2D transitions is the modification of magnetic anisotropy leading to a reorientation of the easy axes. Presiding over the long-range magnetic-order, anisotropies are extremely important in technological applications. For instance, the perpendicular reorientation taking place in many ultrathin films has often been mentioned in relation to achieving ultradense packing of magnetic bits.

Several examples of magnetic reorientation in thin films have been reported in the last decades.[3] Aside from applicative considerations, the reorientation region is of special interest from a fundamental point of view, namely, because the long-range magnetic order is, in principle, undecided here. Experimental observations address a wide variety of cases, ranging from the complete loss of long-range magnetic order,[4] to the formation of complex and sometimes metastable domains,[5,6] to cases in which, close to the critical thickness, novel ordered structures involving mesoscopic domain patterns (e.g., stripes, bubbles, etc) take place.[7]

A well-known example of magnetic reorientation occurs in Fe(110) films.[8–10] The easy axis of thin Fe(110) films is along the $[1\bar{1}0]$ direction and the bulk [001] easy axis is recovered only for thick films.[11] The critical thickness (t_R) of this 90° *in-plane* magnetic reorientation transition is ~70 Å at room temperature. The same reorientation can be thermally induced; the [001] magnetization of a thick film reorient along the $[1\bar{1}0]$ direction with increasing temperature.[12] Much work has been devoted to the study of the Fe(110) reorientation transition, focusing the attention on dependences on temperature,[13] surface capping,[14] chemisorption,[15] electron-beam stimulation,[16] and alloying with other transition metals.[17] However, important information at the microscopic scale is still lacking. For example, laterally averaging techniques cannot distinguish between reorientation via domain opening rather than through a continuous rotation of spins.[18]

In this study the Fe(110) reorientation transition is investigated using x-ray magnetic circular dichroism-photoemission electron microscopy (XMCD-PEEM). Fe(110) uniform films and wedge-shaped samples, encompassing the critical thickness t_R, are examined. The microscopic analysis reveals the existence of two distinct length scales concurring to determine the magnetic boundary region. At the nanoscale, the reorientation takes place abruptly (first-order transition): regions oriented along the [001] and $[1\bar{1}0]$ axes directly meet through thin domain lines. Transversally, however, micron-size faceting structures characterize the morphology of the magnetic boundary. Furthermore either straight or sawtoothed boundaries are formed, depending on the macroscopic direction of the reorientation relative to the crystallographic axes. This effect implies the possibility of manipulating the sharpness of the reorientation transition by appropriate selection of this direction. The order of the reorientation transition is controlled by surface and bulk anisotropies whereas its roughness at the microscopic scale is a direct consequence of long-range magnetostatic interactions.

II. EXPERIMENTAL AND DISCUSSION

The experiments were performed with the SPELEEM microscope at the Nanospectroscopy beamline (Elettra, Trieste, Italy).[19] The W(110) substrate was prepared by repeated cycles of annealing in oxygen atmosphere ($T=1400$ K, $p_{O_2}=1\times10^{-6}$ Torr) and subsequent flashes at high temperature. All experiments were conducted in ultrahigh-vacuum conditions (base pressure $\sim2\times10^{-10}$ Torr). Fe films were prepared *in situ* using an e-beam source; the W(110) substrate was kept at room temperature and the base pressure raised to $\sim1\times10^{-9}$ Torr during deposition. Linear microwedge samples were formed by placing a knife edge between the substrate and the Fe source. Additionally conical microwedges were obtained by evaporating Fe through a 30 μm pinhole aperture.

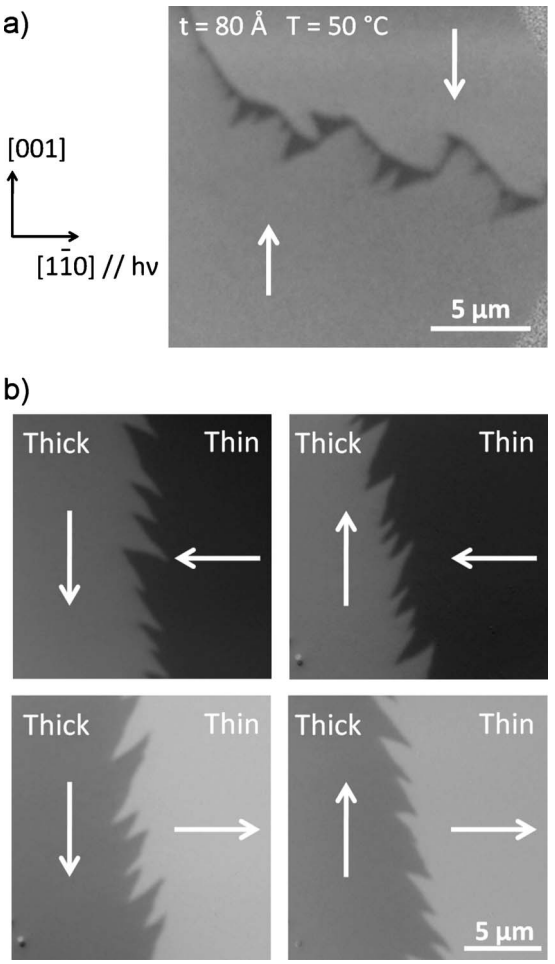

FIG. 1. (a) XMCD-PEEM image from a 80 Å uniform Fe(110) film at the onset of the temperature-induced reorientation transition occurs (~50 °C). Image horizontal coincides with the [1$\bar{1}$0] axis, which is nearly parallel to the photon beam direction. White arrows mark the orientation of the large [001] domains. (b) XMCD-PEEM closeup view of the thickness-induced magnetic reorientation transition. Inverting the magnetization of the thick domain (top and bottom row) causes a 90° flip of the triangular boundary.

Figure 1(a) shows an XMCD-PEEM image from a 80 Å uniform Fe(110) film. At room temperature, the sample contains only [001] domains, separated by barely detectable domain walls. The two oppositely oriented domains display slightly different shadows of gray due to a small sample misalignment, resulting in a remnant magnetization component along the x-ray beam. Taken at approximately 50 °C, Fig. 1(a) captures the starting of the temperature-induced magnetic reorientation. The initially thin wall separating the two oppositely oriented domains (white arrows) expands into triangular regions accommodating the 90° rotated domains (black triangles). The triangles are distributed unevenly on the two sides of the boundary line. Triangles pointing down alternate with triangles pointing up, originating from approximately orthogonal segments.

The thickness-induced magnetic reorientation is shown in Fig. 1(b). The images are taken on a microwedged Fe(110) film spanning the critical reorientation thickness. The thickness gradient is along the horizontal line and the estimated wedge steepness is ~1 Å/μm. Although the average direction of the magnetic boundary is perpendicular to the thickness gradient, the boundary has a sawtooth morphology, with triangular edges extending over a region of approximately 3 μm, corresponding to about 2 Fe monolayers equivalent. The triangle vertices open with an angle of ~35°–40°.

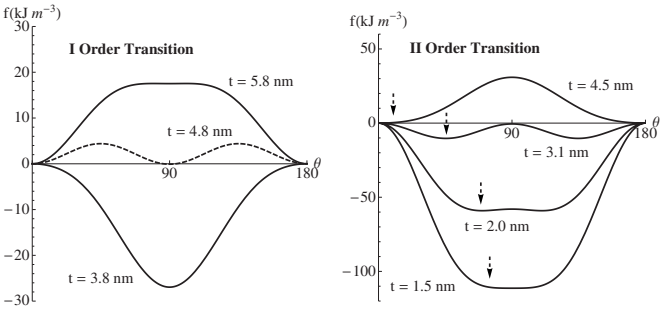

FIG. 2. Anisotropy energy density curves vs magnetization angle (θ) away from the [001] direction. Controlled by the specific values of the material anisotropy constants, first-order (left, Fe metal) and second-order transitions (right) can be induced varying the film thickness.

Apparently the 90° switch of the magnetization happens abruptly without passing through any other intermediate direction. The first-order character of this transition is consistent with Fe magnetic anisotropies.[8] For bcc-(110) films, the total in-plane anisotropy energy density—combining magnetocrystalline, magnetoelastic and surface contributions—is well described by $f_{\parallel}=A\sin^2(\phi)+B\sin^4(\phi)$. ϕ is the magnetization angle away from the [001] direction and the first- and second-order anisotropy constants are the sum of volume and surface terms: $A=K_v-K_s/t$ and $B=K_v'-K_s'/t$, with t the film thickness. The energy density appropriate for Fe(110) films prepared at room temperature is displayed in the left panel of Fig. 2. At the critical thickness (t_R=4.8 nm, dashed line), the [001] and the [1$\bar{1}$0] directions (0° and 90°, respectively) constitute equivalent relative minima. A first-order transition can therefore be expected.

Interestingly these calculations show that the order of the transition can be readily controlled. Artificially increasing the second-order surface anisotropy constant, for example, results in the situation depicted in Fig. 1, right panel. In this case a precise critical thickness cannot be defined. Rather a range of thicknesses exists (between approximately 1.5 and 4.5 nm in Fig. 1) in which the two high-symmetry orientations are both relative maxima. In this range, a third, intermediate magnetization direction becomes the stable solution, describing a continuous rotation of the magnetization (i.e., second-order transition).[20] The corresponding case for the Fe/W(110) can be found in Ref. 18, in which an in-plane transition proceeds via a continuous rotation of the magnetization as a result of the presence of a Au interlayer.

The above considerations based on the anisotropy energy cannot account for the shape of the magnetic boundary at the microscopic scale [see Fig. 1(b)]. Such sawtooth patterns, usually observed for head-on domains, result from magnetostatic interactions.[21] Consistently the sawtooth orientation switches when the relative magnetic alignment reverses [see

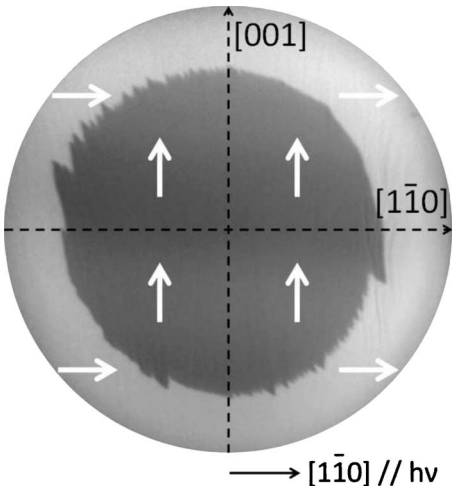

FIG. 3. XMCD-PEEM image of the magnetic reorientation transition in an Fe(110) conical wedge, epitaxially grown on W(110). The diameter of central dark region is about 21 μm.

Fig. 1(b)]. Additionally a similar observation was reported for Fe/GaAs(110) and briefly attributed to magnetostatics.[16]

To further elucidate the origin of the sawtooth boundary, films were grown in the form of conical microwedges. In this configuration, all possible directions of the reorientation transition with respect to the crystallographic axis are realized in a single sample. The resulting XMCD-PEEM micrograph (Fig. 3) demonstrates that the boundary faceting strongly depends on the orientation of the wedge with respect to the crystallographic axes. Out of the four quadrants marked in the figure, two of them feature sharp, filiform boundaries, while the other two display zigzag patterns extending over a few microns. These observations imply the existence of a preferential direction with minimum cost for the domain boundary. When the reorientation is forced along a different direction, the domain boundary spontaneously brakes into triangular patterns in an attempt to minimize the boundary length along unfavorable magnetic directions.

The mechanism leading to the observed triangular deformations is the reduction of the total *magnetic charge* at the boundary.[21] The effect can be demonstrated by employing a simple model of a disk divided into two equivalent domains (semicircles) of uniform, orthogonal magnetizations [see inset in Fig. 4(a)]. The calculated energy costs as a function of boundary orientation are displayed in Fig. 4(a). The short range interaction (continuous line), representing nearest-neighbor exchange, displays two symmetric minima along the bcc(110) close-packed directions, corresponding to the maximum number of lattice sites disrupted by the magnetic boundary. The long-range interaction (dashed line), due to the dipolar energy, shows instead a pronounced left-right asymmetry arising from the angular dependence of the dipole-dipole interaction. The dipolar energy curve implies therefore a preferred angular direction for a magnetic boundary [e.g., −45° in the geometry of Fig. 4(a)]. When the magnetic boundary is forced along a different, higher energy direction, a triangular sawtooth pattern sets in to relieve this situation. Furthermore, precisely as observed, this model predicts a 90° reversal of the sawtooth wave, when one of the two magnetizations is switched.

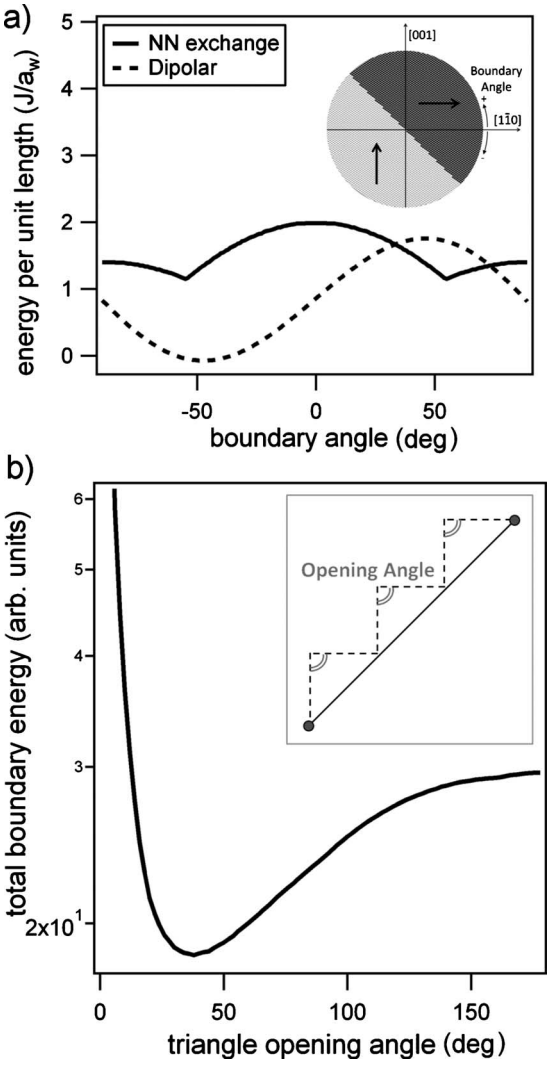

FIG. 4. (a) Angular dependences of NN-exchange and long-range dipolar interactions for the boundaries along the disk diameters. (b) Boundary energy as a function of triangular distortion as sketched in the inset (180° corresponds to no distortion).

The concept of an energetically unfavorable boundary evolving into a sawtooth shape is further illustrated in Fig. 4(b). Starting from the boundary direction with the highest energy cost (+45° in our case), the triangular distortion gives a lower boundary energy per length. This is balanced with the increase in the boundary length, resulting in an optimum configuration. In the distorted boundary the *opening angle* at the apex of the triangles depends on the ratio of dipolar to exchange interaction strengths. The experimentally observed opening angle, distributed in a range from 35° to 40°, is reproduced in Fig. 4(b) for a g/J ratio of the order unity. The variation in experimentally measured angles likely stems from pinning sites, which were also observed to have a strong influence on the propagation of the boundary upon thermal stimulation.

The model above explains successfully the mechanism for forming the sawtooth boundary, however, gives little clue regarding the length scale (i.e., extent of triangles). In practice this is probably strongly influenced by the presence of

defects acting as domain pinning sites and is therefore difficult to assess quantitatively. In an ideal case, however, a constraint on the minimum triangle length may be determined by the increased packing of neighboring domain walls and the corresponding interaction energy.

III. CONCLUSION

In conclusion, at the nanoscale the in-plane spin-reorientation transition in clean Fe on W(110) is a first-order transition with sharp boundaries separating regions of orthogonal magnetizations. On the micron scale, however, long-range dipolar interactions become dominant resulting in characteristic boundary faceting with triangular morphology. The phenomenon takes place according to the average direction of the reorientation with respect to the crystallographic axes. The microscopic roughness of the magnetic boundary is therefore to some extent under control by proper choice of the thickness gradient of the wedge-shaped Fe film. It is interesting to note that the mechanisms shown to operate in the formation of these *magnetic charge walls* can be applied to phenomena observed in other systems due to the general form of the interactions considered. In particular, electrostatic or elastic systems may show similar phenomena due to a competition of the short- and long-range forces analogous to the current study.[22–24]

ACKNOWLEDGMENTS

NSLS is supported by the U.S. Department of Energy under Contract No. DE-AC02-76CH00016.

[1] C. A. F. Vaz, J. A. C. Bland, and G. Lauhoff, Rep. Prog. Phys. **71**, 056501 (2008).
[2] S. Blügel, Phys. Rev. Lett. **68**, 851 (1992).
[3] *Ultrathin MagneticStructures: I,II*, edited by J. A. C. Bland and B. Heinrich (Springer, Berlin, 1994).
[4] D. P. Pappas, K.-P. Kämper, and H. Hopster, Phys. Rev. Lett. **64**, 3179 (1990).
[5] Z. Q. Qiu, J. Pearson, and S. D. Bader, Phys. Rev. Lett. **70**, 1006 (1993).
[6] Y. Millev and J. Kirschner, Phys. Rev. B **54**, 4137 (1996).
[7] A. B. MacIsaac, K. De'Bell, and J. P. Whitehead, Phys. Rev. Lett. **80**, 616 (1998).
[8] H. J. Elmers and U. Gradmann, Appl. Phys. A: Mater. Sci. Process. **51**, 255 (1990).
[9] G. A. Prinz, G. T. Rado, and J. J. Krebs, J. Appl. Phys. **53**, 2087 (1982).
[10] U. Gradmann, J. Korecki, and G. Waller, Appl. Phys. A: Mater. Sci. Process. **39**, 101 (1986).
[11] This behavior seems to be quite generally associated with Fe(110) films; it has been observed for Fe(110) films epitaxially grown on such different substrata as W(110).
[12] The transition is reversible only for a limited range of temperature ($T<400$ °C). At higher temperatures the film undergoes irreversible transformations with considerable mass transport and leading eventually to the formation of characteristic nanowires.
[13] O. Fruchart, J. P. Nozieres, and D. Givord, J. Magn. Magn. Mater. **165**, 508 (1997).
[14] H. J. Elmers and U. Gradmann, Surf. Sci. **304**, 201 (1994).
[15] I.-G. Baek, H. G. Lee, H.-J. Kim, and E. Vescovo, Phys. Rev. B **67**, 075401 (2003).
[16] T. L. Monchesky, J. Unguris, and R. J. Celotta, J. Appl. Phys. **93**, 8241 (2003).
[17] H. Lee, I.-G. Baek, and E. Vescovo, Appl. Phys. Lett. **89**, 112516 (2006).
[18] R. Zdyb, T. O. Menteş, A. Locatelli, M. A. Niño, and E. Bauer, Phys. Rev. B **80**, 184425 (2009).
[19] A. Locatelli, L. Aballe, T. O. Mentes, M. Kiskinova, and E. Bauer, Surf. Interface Anal. **38**, 1554 (2006).
[20] H. Horner and C. M. Varma, Phys. Rev. Lett. **20**, 845 (1968).
[21] A. Hubert and R. Shaefer, *Magnetic Domains: The Analysis of Magnetic Microstructures* (Springer-Verlag, Berlin, 1998).
[22] J. B. Hannon, N. C. Bartelt, B. S. Swartzentruber, J. C. Hamilton, and G. L. Kellogg, Phys. Rev. Lett. **79**, 4226 (1997).
[23] J. P. Pelz, C. Ebner, D. E. Jones, Y. Hong, E. Bauer, and I. S. T. Tsong, Phys. Rev. Lett. **81**, 5473 (1998).
[24] J. B. Hannon, N. C. Bartelt, B. S. Swartzentruber, J. C. Hamilton, and G. L. Kellogg, Phys. Rev. Lett. **81**, 5474 (1998).